High temperature machines: A comparison between ceramic-coated wires and anodized aluminum strips

Daniel Roger, Gabriel Vélu, Sonia Ait-Amar, Sylvain Babicz

HIGH TEMPERATURE MACHINES: A COMPARISON BETWEEN CERAMIC-COATED WIRES AND ANODIZED ALUMINUM STRIPS

Daniel Roger, Gabriel Vélu, Sonia Ait-Amar*, Sylvain Babicz
Univ. Artois, UR 4025, Laboratoire Systèmes Electrotechniques et Environnement (LSEE)
FSA, Technoparc Futura, F-62400, Béthune – France
sonia.aitamar@univ-artois.fr

Abstract—**The paper proposes a comparative approach of two wire technologies for making compact coils able to operate in high temperature (HT°) machines. The first technology is based on ceramic-coated round wire associated with a HT° cement. The second one uses anodized aluminum strips. The advantages and drawbacks of the two technologies are compared, considering the machine global performances at high temperatures.**

Keywords—High temperature machine, Inorganic insulation, Thermal equivalent circuits.

I. INTRODUCTION

Electrical machines are widely used in industry and transports; they perform efficient and accurate controls of complex mechanical systems. This advantage is however limited by their maximal running temperature, which is directly linked to the thermal limits of the polymers used in the electrical insulation system (EIS) and the expected lifetime [1-4]. Consequently, classic electrical machines cannot work in very hot environments, where the temperature exceeds 200 °C as, for instance, near an aircraft turbine. Design of machines able to work permanently under high internal temperatures (over 250°C), is nevertheless possible with inorganic EIS made without any polymers [5,6]. These high temperature machines are designed with rigid coils made with ceramic coated wires and HT° cements used as potting materials. Such coils are able to withstand 500°C. For HT° machines, the design process is very different than for classical ones, because the inorganic coils are rigid objects. The magnetic core must be adapted to rigid coils. Distributed windings with complex end-winding connections are very difficult to build.

Generally speaking, the rated power of an electrical machine depends on the rotor speed, the flux density in the air-gap and the current density in active conductors [7,8]. The same principles apply for HT° machines, but with higher current densities because of the higher internal temperature gradients. The heat flows are more intense for the same motor sizes. The comparative study relies on a simplified thermal model, which computes the temperature of the critical parts of the machine.

II. COMPARISON PRINCIPLE OF THE WINDING TECHNOLOGIES

The assessment of the power density differences due to the two HT° insulation technologies is performed considering two identical Permanent Magnet Synchronous Machines (PMSM). The rotors are equipped with the same surface-mounted high-performance magnets. The only difference is the stator coil technology. Both machines are made using the widespread “24 teeth / 20 poles” structure for high power density applications [9]. Each stator tooth receives a prefabricated coil. All coils have the same number of turns. The 24 stator coils form 3 phases of 8 coils connected in series. The winding directions are chosen to get a dominant 20-pole rotating field in the air-gap, when a balanced 3-phase system feeds the machine. Fig. 1 shows the stator of the machine made with ceramic-coated wire coils embedded in a HT° potting cement. The general aspect of the stator made with anodized aluminum strips is very similar. This figure shows also the details of two consecutive inorganic coils on stator teeth. The coils have a rectangular cross section. The slots are cuboid and the teeth faces are parallel. Consequently, the slots have a specific shape with a larger width in their bottom that cannot be used by the coils. The small additional teeth in the bottom of the slots yield a better thermal contact between the coils and the magnetic core. Another solution will be to make not cubic coils but with a trapezoidal section, to feel all the slot. In this case pair and unpair coils are different and more complexe to wind previously.

Fig. 2 shows the details of the first tested technology for building inorganic HT° coil made with round ceramic-coated wire. The turn distribution presented in Fig. 2 is schematic; it represents the worst case. In a real coil, the external layer is wound with a tensile force on the wire. The turns apply a mechanical pressure that bends the inter-layer insulation mica film. Therefore, the real thermal contact between layers is slightly better than in the model. For this example, a two layer 19-turn coil is considered. The mica inter-layer insulation must be added because of the poor electrical performances of the ceramic coating [10]. The ground insulation is also made of mica. A potting HT° cement immobilizes the turns and the mica. The hardening thermal cycles of the cement are made in a steel mold. Therefore, the coils are rigid objects with a good mechanical accuracy given by the mold and with a high mechanical hardness. They are placed on stator teeth with a small clearance of more or less 0.1mm. The slot is closed with a non-magnetic thin steel wedge. A HT° textile strip is placed between the rigid coil and the wedge for getting a mechanical clamping. The alternative HT° technology is presented in Fig. 3. The coil is made with anodized aluminum strip. The alumina layer obtained by the anodization

process is 5 µm thick [11]. The position of each turn is very different; the voltage distribution between turns is much better [12]. The mica ground insulations and the potting cement are identical.

III. BASIS OF THE COMPARISON

For comparing the two inorganic coil technologies, it is supposed that the coil external geometries and the number of turns are identical. Same stators are modeled with the same teeth and slot sizes. The internal temperatures are computed for identical external temperatures and the same global current. The reference is the round wire technology. The coil is made of 19 turns of ceramic-coated wire. For high temperatures, the copper must be protected by a nickel layer of $40\mu m$. The metal diameter is 1.6mm. The coating thickness is in the range of 10-15µm. It is also supposed that an extra space between adjacent turns exists, because of the difficult winding with a brittle ceramic insulated wire. Consequently, the distance between the metal surfaces of two adjacent turns is estimated to 200µm. With these hypotheses the coil thickness is $th = 4.3mm$; the height of the coil is $h = 18.6mm$, taking into account the thickness of the mica ground insulation. The global cross section of this rectangular coil is $80\ mm^2$ for an effective conducting section of $38.2\ mm^2$. The feeling ratio is estimated to 47%, which suppose a careful winding.

When the alternative anodized-aluminum technology is used to build the same coil, it requires a careful potting. Therefore, it is necessary to have a sufficient space between the mica insulation and the anodized-aluminum strip, which must be filled by the HT° cement and is estimated to 200µm. Consequently, the strip height is $17mm$. The cumulated thickness of the 19 strips is $3.18mm$. Therefore, the anodized-aluminum strip thickness must be $167\mu m$ with the alumina insulation and $157\mu m$ without. The global conducting section is $50\ mm^2$, the feeling ratio of the coil is better (62,5%).

IV. THERMAL COMPARISON

The simplified thermal equivalent circuit of Fig. 4 is used for estimating the motor internal temperatures. The model is based on four simplifying hypotheses:

- The thermal flows between nodes are proportional to the temperature differences;
- Only 4 temperatures in critical parts are considered: the rotor magnets (M), the windings (W), the stator core (Iron-I) and the motor frame (F);
- The cooling system is a standard fan that creates an external airflow through the fins of the stator frame;
- The direct heat exchange between coils is neglected.

The magnets are glued on a metallic rotor. Consequently, a part of the magnet losses (P_M) flows directly outside the motor by the metallic shaft (G_{MA}). The other part crosses the air-gap toward the stator (G_{MW} and G_{MI}). The only difference between both coil technologies is the red part of Fig. 4. The aluminum strip technology yields a radial thermal flow in aluminum, higher than the first technology, where the heat flow must cross the cement potting. The red part of the thermal equivalent circuit must be detailed at the turn level.

Generally speaking, for the classical polymer insulation technology, the rated current is obtained when the maximum temperature is reached at the hottest point of the winding insulation. This widespread reasoning is based on a simple fact: if the insulation breaks at the hottest point and a cumulative phenomenon destroys all of the insulation. However, the temperature of the hottest point depends on the life expectancy of the machine estimation are performed using the standards bases on Ahrenius law.

For inorganic insulation technologies, the problem is very different because the potting cement can withstand very high temperatures, over the Curie point of the iron core or aluminum melting point [13]. The rated current must be defined with new concepts. For permanent magnet machines, the rated value can be defined by the maximum temperature of magnets, which is more or less 350°C [14]. The rated value can also be defined considering the decrease of the machine efficiency. A more detailed analysis is proposed for comparing the two proposed organic technologies.

A. Equivalent circuit for round wire technology

The detailed thermal equivalent circuit of the coil is presented in Fig. 5. Each turn corresponds to a node associated to a power source defined by the corresponding joule losses. The node B correspond to the slot back and T the center of a tooth.
Each turn is inside the HT° cement, the heat flow must cross this cement. The thermal model of a single turn considers the cuboid part of cement around the conducting wire, which is the source. Fig. 6 presents the temperature map in the cement and a schematic representation of the power flow for a single wire represented by eight thermal resistances, one per half a face. They have the same value, they are computed considering that the temperature of the copper wire is 1°C, while the border temperature is fixed to 0°C. The thermal flux presented in Fig. 7 is computed by a 2D finite element method, for the HT° cement and for the standard polymer technology. The 8 thermal resistances are computed by integrating the heat flow on half a face and for the average length of a turn considering an imposed temperature difference of $1°K$ for the simulation. The thermal resistances of the flat parts that correspond to the mica ground and inter-layer insulation are calculated and added for computing all the thermal resistances of Fig. 5; results are given in Table 1.

B. Equivalent circuit for the anodized aluminum strip technology

The heat flow toward the slot back in the aluminum coil is very different. The model divider each strip in three parts. The associated nodes are defined at the center of each part as shown in fig. 8. The thermal equivalent circuit is presented in Fig. 9. The horizontal thermal resistances R_1 represent the thermal transfer through the Al_2O_3 insulating layer. The vertical ones correspond to the heat transfer inside the aluminum strip. Each node is associated to the corresponding joule loses. The heat flow crosses the tooth insulation represented by $R_{T,}$ for the tooth and the 19 conductances R_B. Table 2 gives the thermal resistances.

C. Temperature computation

A PSpice simulator computes the temperature in each node of the equivalent circuits from the joule losses P_T in each turn and the thermal resistances, using the algorithm of fig. 10.

$$(1 R_T I = {}_T P \quad)^2$$

The current I_T is the same for all the turns, but the turn resistances R_T depend on their temperatures. The stator core temperature depends on the whole machine thermal balance, the comparison of coil technologies is not easy in this global context. For comparing easily the HT° coil technologies, the slot back temperature (node B) is arbitrary fixed to 100°C. The algorithm stops for a temperature difference $\varepsilon < °1C$.

Results are given in Fig. 11. The horizontal axes represent the turn position and the vertical axes the temperatures or losses. Fig. 11 is dawn for $I_T = 40A$; current densities are $20A/mm^2$ in the copper and $15A/mm^2$ for the anodized aluminum strip because of the better volume filling. The larger temperatures of turns 11-19, corresponding to the external layer of the coil, shows that the heat-flow crosses the inner layer. The temperature differences between turns are lower for the cement potting because of its better thermal conductivity. Despite higher joule losses in aluminum turns, the turn temperatures are lower with a negligible difference between turns. A more detailed analysis shows also a very small temperature difference inside aluminum strips, the difference between nodes L, M and H (fig. 8) are under $1°C$, because of the high thermal conductivity of aluminum.

For $40A$, the temperature at the hottest points remains compatible with standard class H polymer insulation systems. However, this technology cannot be used for higher currents. The same algorithm is used for computing temperatures and losses for $80A$ and for inorganic technologies, because the temperatures are too high for polymers. Results are given in Fig. 12. It can be seen that temperatures are much higher than for $40A$ but they remain compatible with the capabilities the potting cement and alumina. These results show that, despite of higher joule losses, the coils made with anodized-aluminum strips can be used for very high currents.

V. Conclusion

For prefabricated coils placed on rectangular teeth, the anodized aluminum technology offers a better filling than round wires. Consequently, the current density is lower for the same stator current. The thermal transfer between the turns and the stator core is better and, despite, the higher joule losses due to the higher resistivity, the average temperatures are similar for the two HT° technologies. With these technologies, it is possible to work with much higher currents, for the same coil volumes that increase strongly the power density when the magnetic core temperature remains at the same value by an efficient cooling system.

References

[1] F. Aymonino, T. Lebey, D. Malec, C. Petit, J. S. Michel, A. Anton, and A. Gimenez, "Degradation and dielectrics measurements of rotating ma- chines insulation at high temperature (200-400°C)", *Proc. of 2007 IEEE International Conference on Solid Dielectrics*. Winchester, UK, pp. 130–133, 2007. •

[2] Standard EIC 60216-1 "Matériaux isolants électrique, Propriétés d'endurance thermique", 2002.

[3] E. Amendola, E, G. Lupò, C. Petrarca, A. M. Scamardella, "Alumina filled silicone nanocomposites for electrical insulation of power rotating machines, " Inter. J. of Appl. Electrom. and Mechan. , vol. 39, no. 1-4, pp. 3-11, 2012

[4] K. Komeza, M. Lefik, X. M. López-Fernández, "Calculations of heat transfer coefficient and equivalent thermal conductivity for induction motors thermal analysis," Inter. J. of Appl. Electrom. and Mechan., vol. 46, no. 2, pp. 375-380, 2014

[5] V. Iosif, D. Roger, S. Duchesne, and D. Malec, "Assessment and improvements of inorganic insulation for high temperature low voltage motors," *IEEE Trans. on Dielectr. and Electr. Insul*., vol. 23, no. 5, pp. 2534–2542, 2016.

[6] V. Iosif, D. Roger, S. Duchesne, and D. Malec, "An insulation solution for coils of high temperature motors (500 deg. c)", *Proc. of IEEE International Conferenceon Dielectrics*, vol. 1, 2016, pp. 297–300. •

[7] J. Chatelain, « Traité d'électricité, d'électronique et d'électrotechnique Machines électriques, » Dunod, Ed., 1984.

[8] J. Pyrhonen, T. Jokien and V. Hrabovcova, "Design of rotating electrical machine," Second edition, Wiley, 2014.

[9] A. Tovar-Barranco, F. Briz, A. L. de Heredia, and I. Villar, “Comparison of permanent magnet synchronous machines with concentrated windings and different rotor configurations”, *Proc. of 19th European Conference on Power Electronics and Applications (EPE’17 ECCE Europe)*, Sept 2017, pp. 1-8. •

[10] D. Roger, M. Toudji, S. Duchesne, and G. Parent, “Concentrated winding machines fed by PWM inverters: Insulation design helped by simulations based on equivalent circuits,” *Proc. of IEEE Conference on Electrical Insulation and Dielectric Phenomenon,* pp. 209–212, 2017.

[11] S. Babicz, S. Ait-Amar, and G. Vélu, “Dielectric Characteristics of an Anodized Aluminum Strip,” *IEEE Trans. Dielectr. Electr. Insul.*, vol. 23, no. 5, pp. 2970-2977, 2016.

[12] D. Roger, V. Iosif, and S. Babicz, “Voltage distribution in inorganic insulation windings for high temperature motors”, COMPEL - The international journal for computation and mathematics in electrical and electronic engineering, 2016, Vol. 35, No. 6, pp. 2074-2086.

[13] Final advanced materials. [Online]. Available : http ://www.final-materials.com/ •

[14] J. Liu and M. Walmer, “Thermal stability and performance data for smco 2:17 high-temperature magnets on ppm focusing structures,” Electron Devices, IEEE Transactions on, vol. 52, no. 5, pp. 899–902, May 2005.

Table 1. Thermal resistances for the coil made with round wire.

Thermal resistances (°K/W)		Polymer potting	HT° Cement potting
Turn-to-turn through the inter-layer insulation	R_1	6.6	2.56
Turn-to-turn in the same layer	R_2	3.3	0.29
Turn to tooth	R_3	5.5	7.1
Turn to slot-back	R_B	5.5	7.1
Tooth center – Slot-back	R_T	0.51	

Table 2. Thermal resistances for the coil made with aluminum strip.

Thermal resistances (°K/W)		HT° Cement potting
Strip-to-strip for 1/3 of the strip	R_1	3.15e-3
Inside the strip between nodes	R_2	1.17
1/3 strip to tooth	$R_{TL,M\ or\ H}$	1.03
Strip to slot-back	R_B	55.1
Tooth center – Slot-back	R_T	0.51

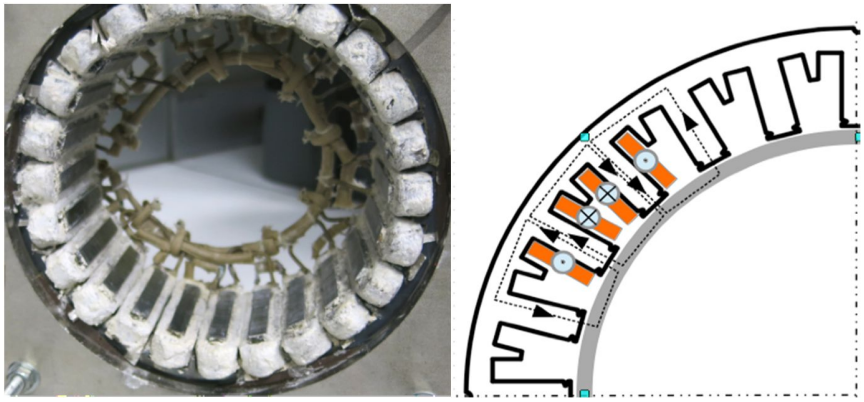

Fig. 1. Stator of a HT° PMSM made with 24 rigid inorganic coils. The picture was made before closing the slots with metallic wedges.

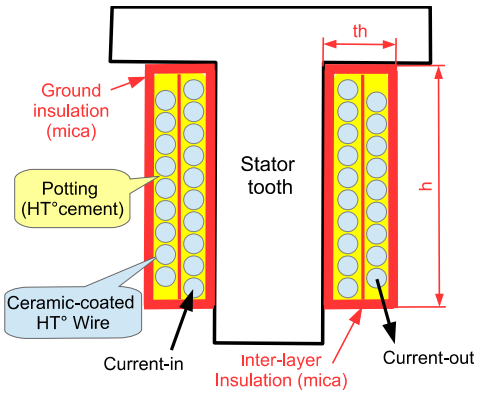

Fig. 2.First technology: ceramic-coated round wire and HT° potting cement.

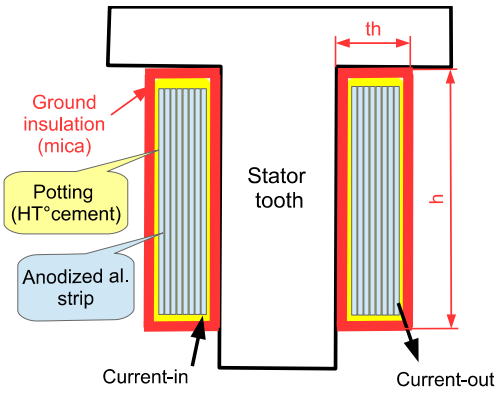

Fig. 3. Alternative technology: anodized aluminum strip and HT° potting cement.

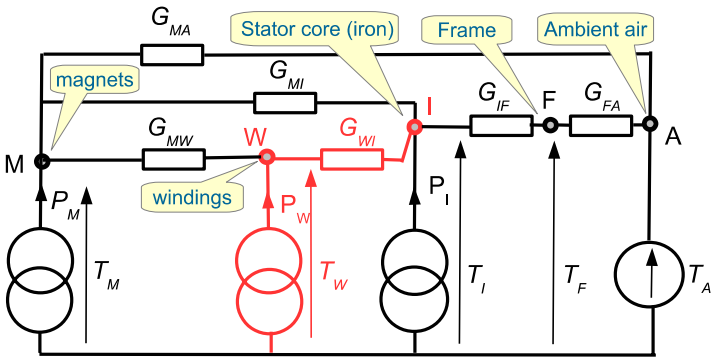

Fig. 4. Simplified thermal equivalent circuit of a PMSM at steady state (P_M=magnet losses, P_W=winding losses, P_I=Iron losses).

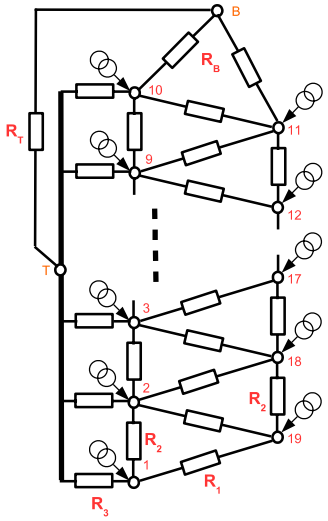

Fig. 5. Detailed thermal equivalent circuit for the coil made with a round wire.

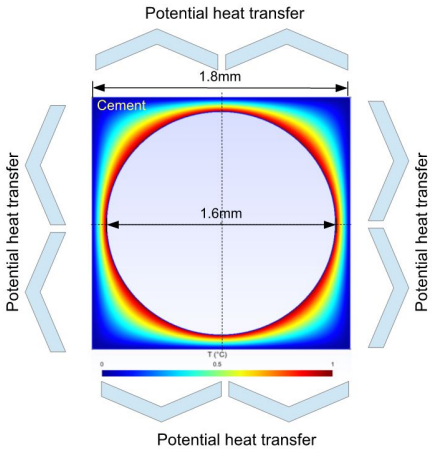

Fig. 6. Round wire thermal simulation for estimating the 8 thermal resistances characterizing the thermal flow.

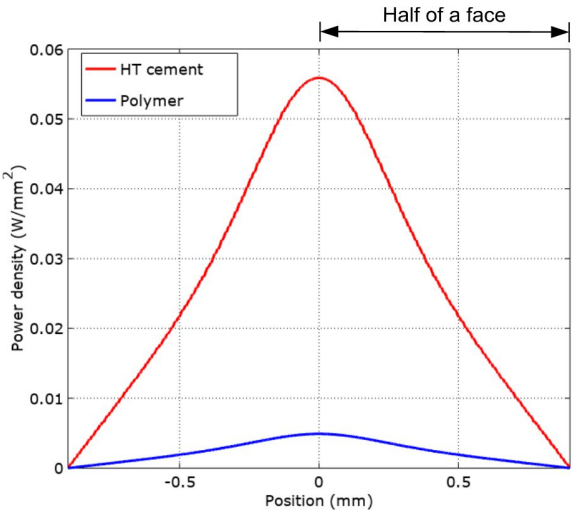

Fig. 7. Power flow through a face of the cuboid-shaped cement around the round wire. The wire temperature is set to 1°C and the cuboid faces to 0°C.

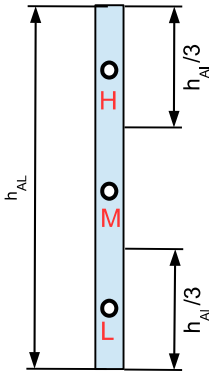

Fig. 8. Position of nodes for the coil made with anodized aluminum strip.

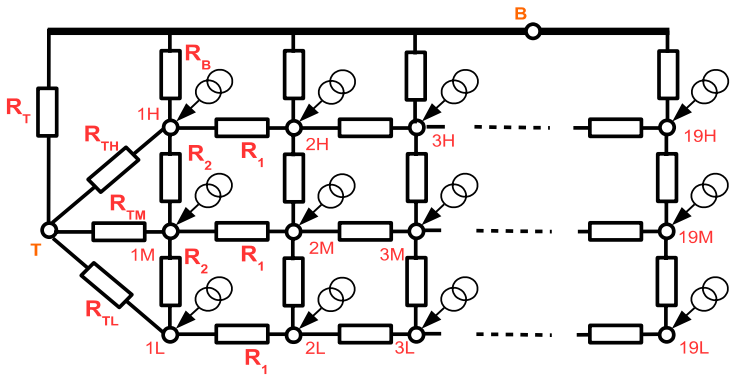

Fig. 9. Detailed thermal equivalent circuit for the coil made with anodized aluminum strip.

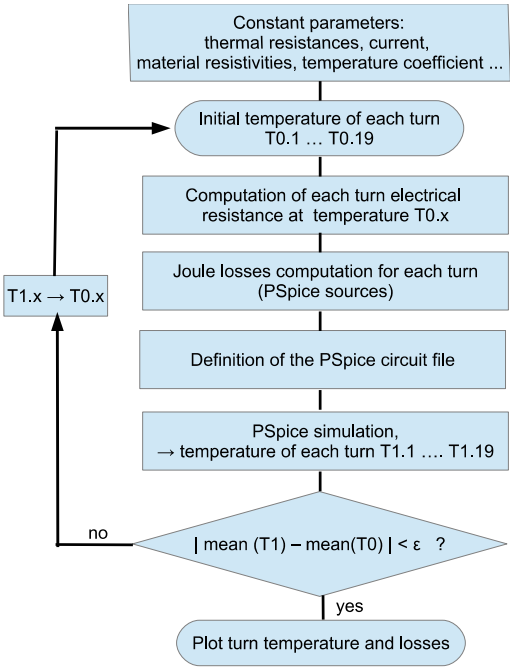

Fig. 10. Computation algorithm with a PSpice simulator.

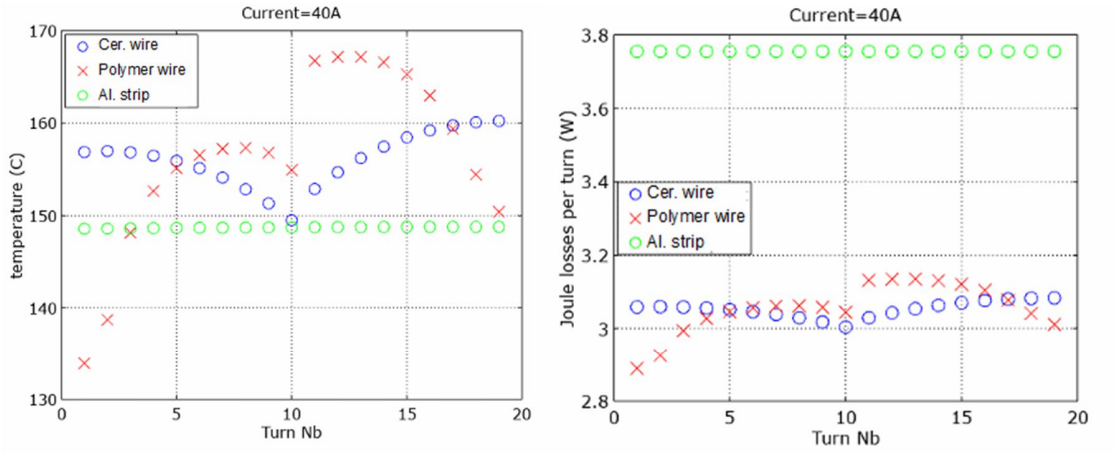

Fig. 11. Temperature and joule losses in every turn for 40A.

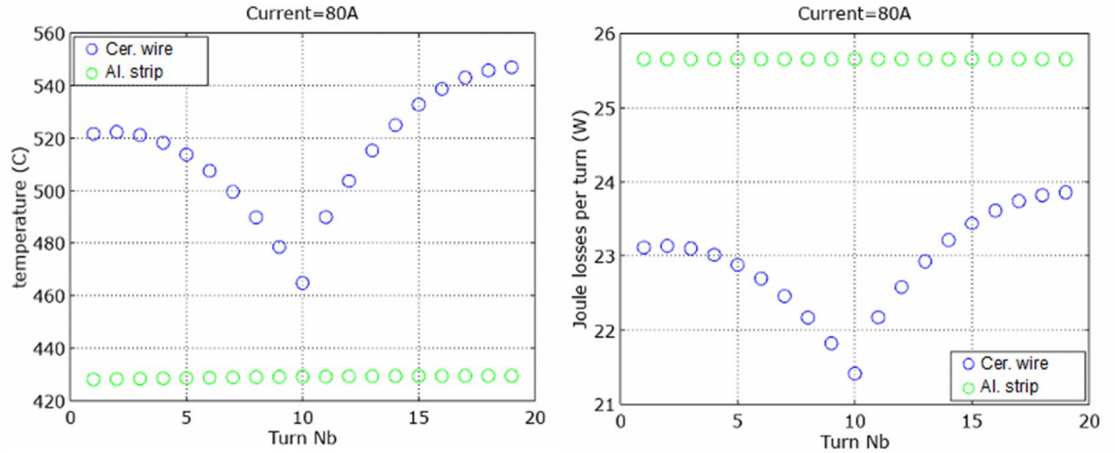

Fig. 12. Temperature and joule losses in every turn for 80A.